



TOPICAL REVIEW

Computational electron–phonon superconductivity: from theoretical physics to material science

To cite this article: Shiya Chen *et al* 2025 *J. Phys.: Condens. Matter* **37** 023002

View the [article online](#) for updates and enhancements.

You may also like

- [Thermal transport in C₆N₇ monolayer: a machine learning based molecular dynamics study](#)
Jing Wan, Guanting Li, Zeyu Guo et al.
- [Non-equilibrium dynamic hyperuniform states](#)
Yusheng Lei and Ran Ni
- [Isolation and characterisation of monolayer phosphorene analogues](#)
Nicolas Gauriot, Raj Pandya, Jack Alexander-Webber et al.

Topical Review

Computational electron–phonon superconductivity: from theoretical physics to material science

Shiya Chen¹, Feng Zheng^{2,*} , Zhen Zhang³ , Shunqing Wu¹ , Kai-Ming Ho³, Vladimir Antropov⁴ and Yang Sun^{1,*} 

¹ Department of Physics, Xiamen University, Xiamen 361005, People's Republic of China

² School of Science, Jimei University, Xiamen 361021, People's Republic of China

³ Department of Physics and Astronomy, Iowa State University, Ames, IA 50011, United States of America

⁴ Ames National Laboratory, U.S. Department of Energy, Ames, IA 50011, United States of America

E-mail: fzheng@jmu.edu.cn and yangsun@xmu.edu.cn

Received 22 July 2024, revised 12 September 2024

Accepted for publication 30 September 2024

Published 18 October 2024



Abstract

The search for room-temperature superconductors is a major challenge in modern physics. The discovery of copper-oxide superconductors in 1986 brought hope but also revealed complex mechanisms that are difficult to analyze and compute. In contrast, the traditional electron–phonon coupling (EPC) mechanism facilitated the practical realization of superconductivity (SC) in metallic hydrogen. Since 2015, the discovery of new hydrogen compounds has shown that EPC can enable room-temperature SC under high pressures, driving extensive research. Advances in computational capabilities, especially exascale computing, now allow for the exploration of millions of materials. This paper reviews newly predicted superconducting systems in 2023–2024, focusing on hydrides, boron–carbon systems, and compounds with nitrogen, carbon, and pure metals. Although many computationally predicted high- T_c superconductors were not experimentally confirmed, some low-temperature superconductors were successfully synthesized. This paper provides a review of these developments and future research directions.

Keywords: superconductivity, material discovery, computational material science

1. Introduction

Searching for room-temperature superconductivity (SC) is recognized as one of the most significant challenges in modern physics. The discovery of copper–oxygen superconductors in 1986 sparked hope that this long-sought dream might be realized [1]. However, understanding the physics behind these superconductors was proven to be complex, turning this area

into a vast and challenging playground for theoretical physicists. Spin fluctuations, believed to be major contributors to this type of SC, pose significant analytical and computational difficulties [2, 3] due to their wide frequency range, which exceeds that of phonon excitations (<0.2 eV). Consequently, material science analysis of these superconductors is currently not feasible.

In contrast, the electron–phonon coupling (EPC) mechanism of SC, described by the Bardeen–Cooper–Schrieffer (BCS) theory [4], allows for a clearer separation of interactions into the local Coulomb pseudopotential, making

* Authors to whom any correspondence should be addressed.

SC calculations feasible. This theoretical framework facilitated the practical realization of high-pressure SC in metallic hydrogen, as suggested by Abrikosov [5], De Gennes [6], and Ashcroft [7] in the 1960s. However, until around 2015, EPC was not considered the primary mechanism for achieving room-temperature SC. The discovery of superconducting hydrogen compounds under pressure demonstrated that EPC could indeed be a source of room temperature SC, leading to the development and widespread use of computational codes based on the theory that incorporates both electron and phonon spectra of real materials [8–14]. These computational advancements spurred extensive searches for EPC superconducting materials [15], leading to numerous confirmed discoveries such as CaH_6 [16], YH_6 [17], YH_9 [18], and LaH_{10} [19, 20]. A comprehensive review article [21] recently summarized the studies of high-pressure metal superhydrides superconductors up to mid-2023.

The exponential growth in computing power over the past few years, culminating in the advent of exascale computing systems capable of performing 10^{18} calculations per second [22, 23], also enables unprecedentedly fast calculations. These systems, along with many-core architectures in modern CPUs offering high core counts and advanced parallel processing capabilities, are ideal for high-throughput tasks such as searching for SC in millions of materials. In addition, the development of quantum simulators [24, 25] are also advancing the understanding of microscopic origin of SC.

The development of efficient computational schemes for total energy and EPC SC calculations forms the basis for computationally searching for SC. The stability of compounds can now be reasonably evaluated using convex hull and phonon calculations. Crystal structure prediction (CSP) methods such as CALYPSO [26], USPEX [27], AIRSS [28], and high-throughput screening techniques [29–32], enabled researchers to systematically explore extensive configurational spaces to identify stable crystalline structures under pressures. The strength of EPC and T_c can also be directly computed with well-optimized community codes, yielding qualitatively consistent results. Machine learning techniques have been implemented to further accelerate T_c calculations. The workflow and related algorithms for predicting EPC SC are well summarized in a recent review by Pickett [33].

It is now evident that computational material science can reliably predict EPC SC, provided the electronic structure is adequately described. As a result, there is an intense search for high T_c EPC SC under ambient pressures, with a few systems predicted to have T_c values close to or exceeding that of nitrogen in the past year. This review summarizes the newly predicted superconducting systems from 2023 to 2024, focusing on their chemical compositions and structural motifs.

2. Predicted superconductors in 2023–2024

We identified over a hundred papers on computational predictions of superconducting systems from 2023 to 2024 using the

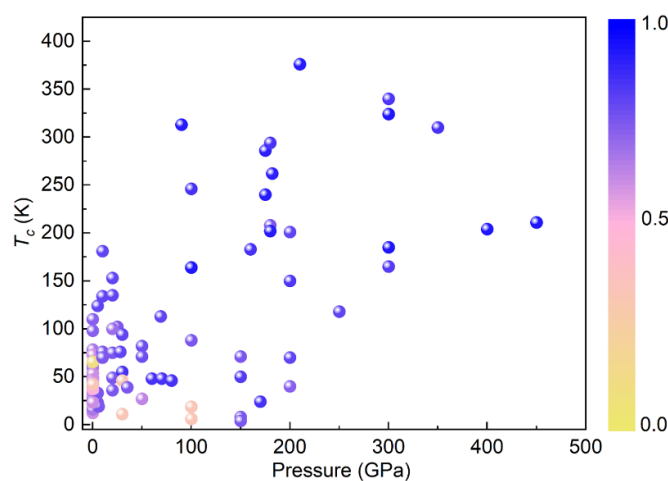


Figure 1. T_c and corresponding pressure of newly reported hydride systems in 2023–2024 [36–60]. The color in the point indicates the H percentage in each compound.

Web of Science database. Our analysis of the chemical compositions revealed that most predicted systems are hydrides, B–C systems, or compounds containing nitrogen, carbon, or pure metal elements. This section classifies and analyzes the motifs of these compounds, grouping them within each category.

2.1. Predictions of hydride superconductors

Figure 1 presents the T_c of newly predicted hydride superconductors at various pressures. It reveals that hydride superconductors in the lower-pressure region have lower hydrogen content and lower T_c compared to those in the higher-pressure region. It was suggested that, at ambient pressure, hydrogen atoms typically exist as H_2 molecules, lacking the metallic properties and strong ionic behavior required for SC [34, 35]. In contrast, at high pressure, systems with higher T_c values undergo the dissociation of hydrogen molecules into hydrogen ions. This pressure-induced change alters the material's electronic band structure, resulting in free electrons and strong electron–ion interactions necessary for SC [33]. Systems with T_c values exceeding 200 K typically have a hydrogen content higher than 0.8.

As shown in figure 2, the hydride superconductors recently predicted under ambient pressure can be classified into three main categories, including the X_2YH_6 system (where X represents rare earth or alkali metals, and Y represents transition or inert metals), the perovskite system (represented by KInH_3), and the $\text{Y}(\text{BH}_4)_2$ system. These three categories share a common structural characteristic: metal and hydrogen atoms form an octahedral packing motif.

2.1.1. X_2YH_6 . The X_2YH_6 system exhibits a face-centered cubic lattice structure, with hydrogen atoms surrounding transition metal atoms to form isolated octahedra. A representative compound, Mg_2IrH_6 , was discovered by Dolui *et al* through

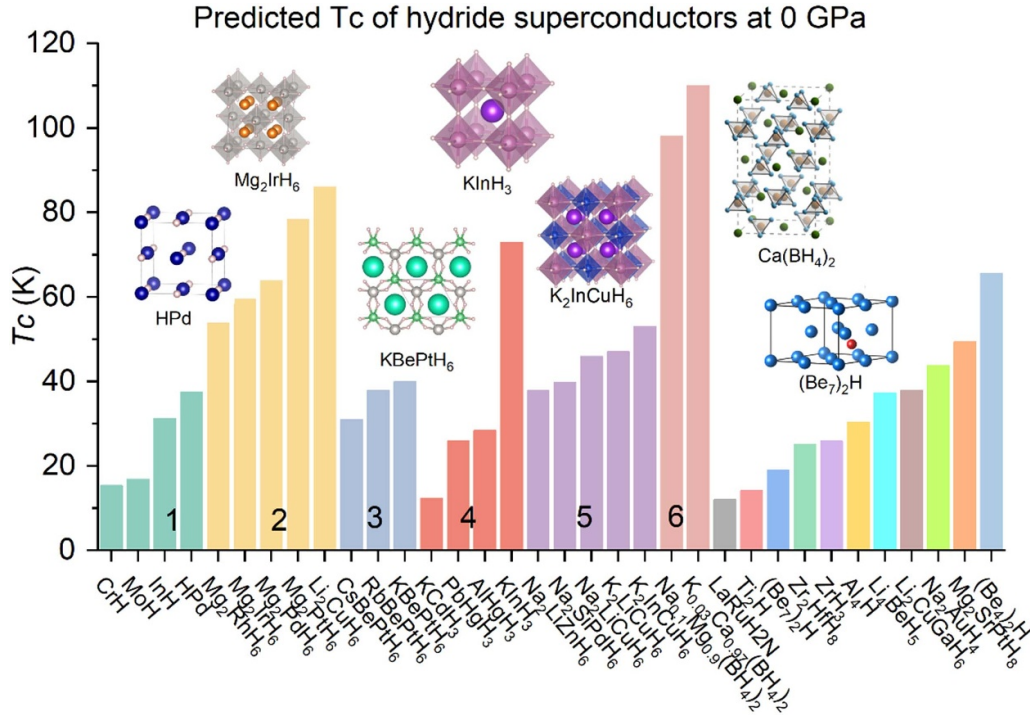


Figure 2. Predicted ambient hydride superconductors in 2023–2024. Different colors in the columns indicate various structural motifs. Data for type 1 come from [36, 37], type 2, type 3, type 4, and type 5 from [37], and type 6 from [57, 65]. The remaining colorful columns correspond to different types of structures, as reported in [36–38].

high-throughput searches of various highly symmetric ternary hydrides [61]. They proposed a feasible synthesis route for Mg_2IrH_6 by first synthesizing the insulating phase Mg_2IrH_7 under high pressure (15 GPa) and then dehydrogenating it. Sana *et al* predicted that Mg_2PtH_6 , belonging to the same structural family, could achieve a T_c exceeding 100 K under ambient pressure with electron doping [62]. Further, Zheng *et al* [63] identified more X_2YH_6 systems, suggesting that these systems exhibit sharp Van Hove singularities at their Fermi levels, contributing to their high T_c . Wang *et al* showed that replacing Mg with Ca resulted in the disappearance of SC in Mg_2IrH_6 , suggesting that the rigid antibonding in the IrH_6 polyhedron may be key to the high T_c in X_2YH_6 systems [64].

2.1.2. Perovskite structure. The ideal perovskite structure, which exhibits cubic symmetry, has been linked to SC since the discovery of the high- T_c superconductor $\text{La}_{2-x}\text{Ba}_x\text{CuO}_4$ by Bednorz and Müller in 1986 [1]. Despite the mechanism still not being fully understood, its T_c far exceeded that of conventional superconductors known at the time, sparking significant exploration in the field.

Recent research focused on perovskite-type superconductors, including the discovery of the non-oxide perovskite superconductor, MgCNi_3 , by He *et al* [66]. Subsequent computational studies confirmed it as a conventional superconductor dominated by strong EPC [67]. In 2023, Tian *et al* predicted the superconducting ternary metal hydride perovskite system, MgHCu_3 [68], with a T_c of 42 K. Figure 2 shows that many perovskite-type conventional superconductors with higher T_c

predicted in the past two years, including the metastable phase KInH_3 [37], which is predicted to have a T_c of 73 K. In these systems, the main contribution to EPC comes from low-frequency phonons induced by heavy atoms, exhibiting diverse electronic band structures and Fermi surfaces [23]. Although several hydride perovskite systems were synthesized, the predicted superconductors were not synthesized [69–71]. Many double perovskite hydride systems were predicted to exhibit SC, theoretically proposed as high-temperature ferromagnetic semiconductors [72], but no system of this type was experimentally synthesized.

2.1.3. $\text{X}(\text{BH}_4)_2$. In figure 2, the doped $\text{Ca}(\text{BH}_4)_2$ system, a molecular crystal where boron and hydrogen form BH_4 tetrahedra, is predicted to exhibit a T_c exceeding 100 K under ambient pressure [65]. Before doping, $\text{Ca}(\text{BH}_4)_2$ is an insulator, and a doping concentration as low as 0.03 holes per formula unit is sufficient to induce a metallic state. The high T_c is attributed to the strong EPC between B–H σ molecular orbitals and bond-stretching phonons. Earlier this year, An *et al* predicted a closely related system, Na-doped $\text{Mg}(\text{BH}_4)_2$ [57], with a T_c reaching 98 K at a doping concentration of 0.1 holes per formula unit, potentially increasing to 140 K with higher doping concentrations. This system shares a similar superconducting mechanism with K-doped $\text{Ca}(\text{BH}_4)_2$. Other metal borohydrides, such as KB_2H_8 [73] and CsB_2H_8 [74], were also predicted to exhibit SC with T_c values of approximately 140 K at 12 GPa and 100 K at 25 GPa, respectively. Due to the wide

commercial availability of metal borohydrides, experimental verification of these systems might be conducted promptly.

Moreover, $(\text{Be}_4)_2\text{H}$ [38], comprising hexagonal layers of Be and B, was predicted to exhibit conventional SC under ambient pressure with an estimated T_c approaching 70 K. However, this system is thermodynamically unstable, posing significant challenges for experimental synthesis and characterization.

2.2. Predictions of B–C superconductors

Figure 3 shows that the newly predicted B–C system superconductors at ambient pressure are primarily represented by two categories. The first extensively studied predicted superconductor, $\text{Li}_{1/2}\text{BC}$ with a T_c above 40 K [75], originates from LiBC through hole doping. Layered LiBC compounds, akin to graphite, long captivated researchers due to their composition of light elements, suggesting strong covalent bonds and distinctive phonon frequencies, which could potentially lead to high-temperature superconducting properties. Their crystal structure resembles the conventional superconductor MgB_2 , exhibiting $P6_3/mmc$ symmetry [76, 77]. Unlike MgB_2 , LiBC is an insulator [77]. Therefore, methods such as hole doping and the introduction of other elements were explored to induce metallicity in LiBC [78–80]. Zheng *et al* extensively investigated the structure and superconducting properties of the Li–B–C system at 100 GPa, discovering that even in many non-layered Li–B–C systems, SC can also be observed [81].

Inspired by the synthesis of SrB_3C_3 under high pressure [88], which shares structural similarities with cage-like hydride superconductors currently under extensive study and is electronically dominated by a covalent B–C sublattice akin to the bonding and electronic properties observed in borides and carbides like MgB_2 , extensive computational studies were conducted to explore its superconducting properties [89–91] and those of similar structures, such as CaB_3C_3 [89] ($T_c = 48$ K at 0 GPa), SrB_4C_2 ($T_c = 19$ K at 0 GPa) [92], $\text{Rb}_{0.4}\text{Sr}_{0.6}\text{B}_3\text{C}_3$ ($T_c = 83$ K at 0 GPa) [93], $\text{Rb}_{0.5}\text{Sr}_{0.5}\text{B}_3\text{C}_3$ ($T_c = 75$ K at 0 GPa) [94] and BaB_3C_3 ($T_c = 43$ K at 0 GPa) [90]. Over the past two years, research on this type of structure continued, exemplified by KPbB_6C_6 [84] ($T_c = 58$ K at ambient pressure). High-throughput screening of all compounds with $Pm\bar{3}$ symmetry, including XB_3C_3 and XYB_6C_6 , revealed relatively high T_c values. It is proposed that the T_c of these compounds can be controlled by adjusting the average valence states of the X and Y metal elements. Duan *et al* predicted that RbBaB_6C_6 and RbYbB_6C_6 could exhibit T_c values of 67 K and 66 K, respectively, at ambient pressure [85]. The matching of the ionic radius of alkaline earth metal elements with the bond length of the cage-like B–C framework is identified as key for the kinetic stability of such compounds under ambient pressure, presenting a new avenue for identifying high-temperature SC in covalent materials under environmentally stable conditions. Moreover, the XB_2C_8 ($X=\text{Na}, \text{K}, \text{Rb}, \text{Cs}$) [86] boron–carbon clathrates, exemplified by CsB_2C_8

(with a predicted T_c of 69 K at 0 GPa), have also been identified as promising high-temperature superconductors. This discovery further expands the family of boron–carbon clathrate superconductors.

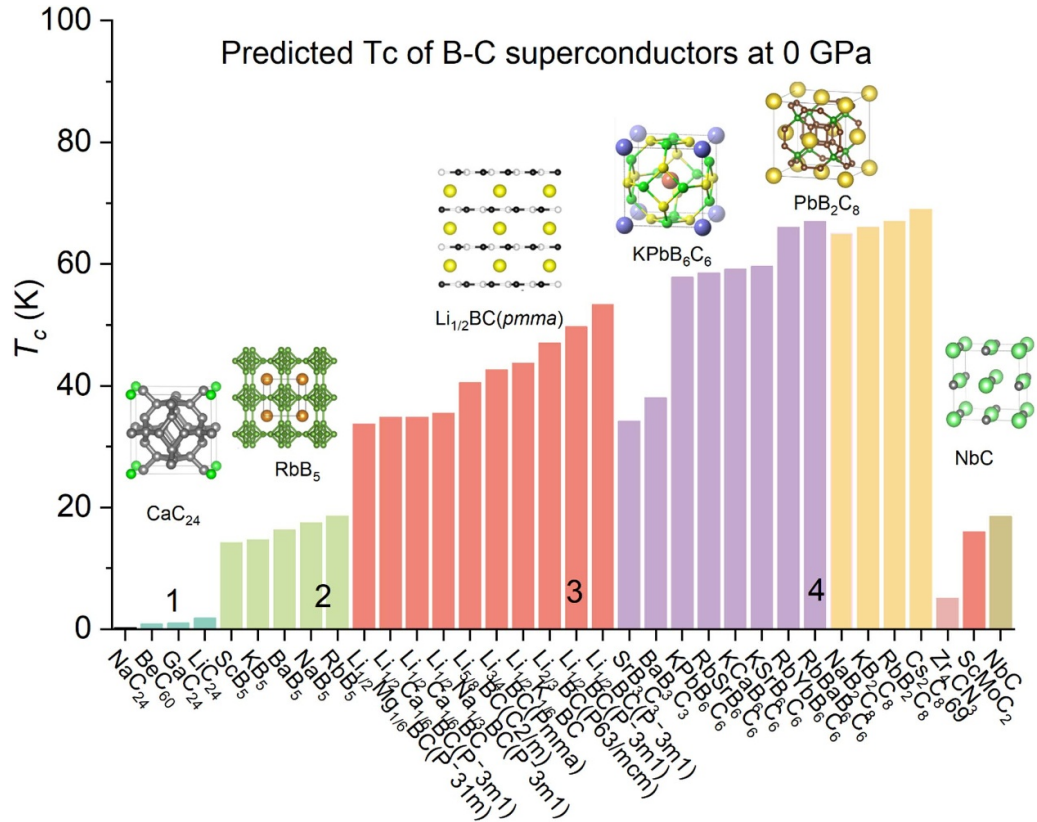
Moreover, Tomassetti *et al* predicted a series of $\text{Mg}_x\text{B}_2\text{C}_2$ and Na_xBC superconductors with T_c ranging from 16 K to 29 K by performing hole doping through thermal deintercalation on MgB_2C_2 and NaBC ternary compounds [95]. Apart from these systems, the predicted T_c of other newly proposed B–C system superconductors does not exceed 20 K. Among them, in the tetragonal crystal structure of pentaborides (XB_5) [83] ($X=\text{Na}, \text{K}, \text{Rb}, \text{Ca}, \text{Sr}, \text{Ba}, \text{Sc}, \text{and Y}$), NaB_5 exhibits the highest T_c of 17 K, whereas the T_c of sodalite-like structured (XC_{24}) [82] ($X=\text{Li}, \text{Na}, \text{K}, \text{Be}, \text{Mg}, \text{Ca}, \text{Al}, \text{Ga}, \text{Ge}$) is below 2 K. These structures all have clathrate-type motifs. Additionally, Chen *et al* performed high-throughput screening on previously synthesized boride compounds and identified TaMo_2B_2 with a T_c of 12 K [30]. At 40 GPa, Yang *et al* predicted that Sr_2B in the $F3m$ structure exhibits a superconducting transition temperature of 105 K [96].

2.3. Other predicted superconductors at ambient pressure

As shown in figure 4, there were a few computational predictions regarding other superconductors, with most systems derived from the work of Cerqueira *et al* [36], who used machine-learning techniques to filter databases based on specific criteria. Among these, LiMoN_2 was predicted to exhibit a T_c of 46 K [36] at ambient pressure, making it the system with the highest predicted T_c at ambient pressure besides hydrides and B–C compounds. This system was experimentally synthesized in 1992 [97], but due to imperfect sample quality and structure, T_c was not observed experimentally. Apart from hydrides and B–C systems, other compounds generally exhibited lower T_c values. It was also observed that most predicted superconductors, apart from hydrides and borides, contained light elements such as C, N, O, and V. This observation aligns with BCS theory [4], where the presence of light elements in materials tended to result in higher Debye temperatures, potentially leading to higher T_c SC.

2.4. Superconducting parameters

The computational calculations provide detailed data to analyze key parameters contributing to the T_c . We selected a few compounds from the X_2MH_6 [63], XB_3C_3 , and XYB_6C_6 families [84] for analysis. Figures 5(a) and (b) summarize the superconducting parameters, including the EPC constant (λ) and logarithmic average frequency (ω_{\log}) for selected X_2MH_6 , XB_3C_3 , and XYB_6C_6 compounds, arranged in order of decreasing T_c . The EPC contributions are divided into cations and H or B/C components. It is evident that cations significantly contribute to λ . In several compounds, the cation contribution to the EPC constant exceeds 30%, and



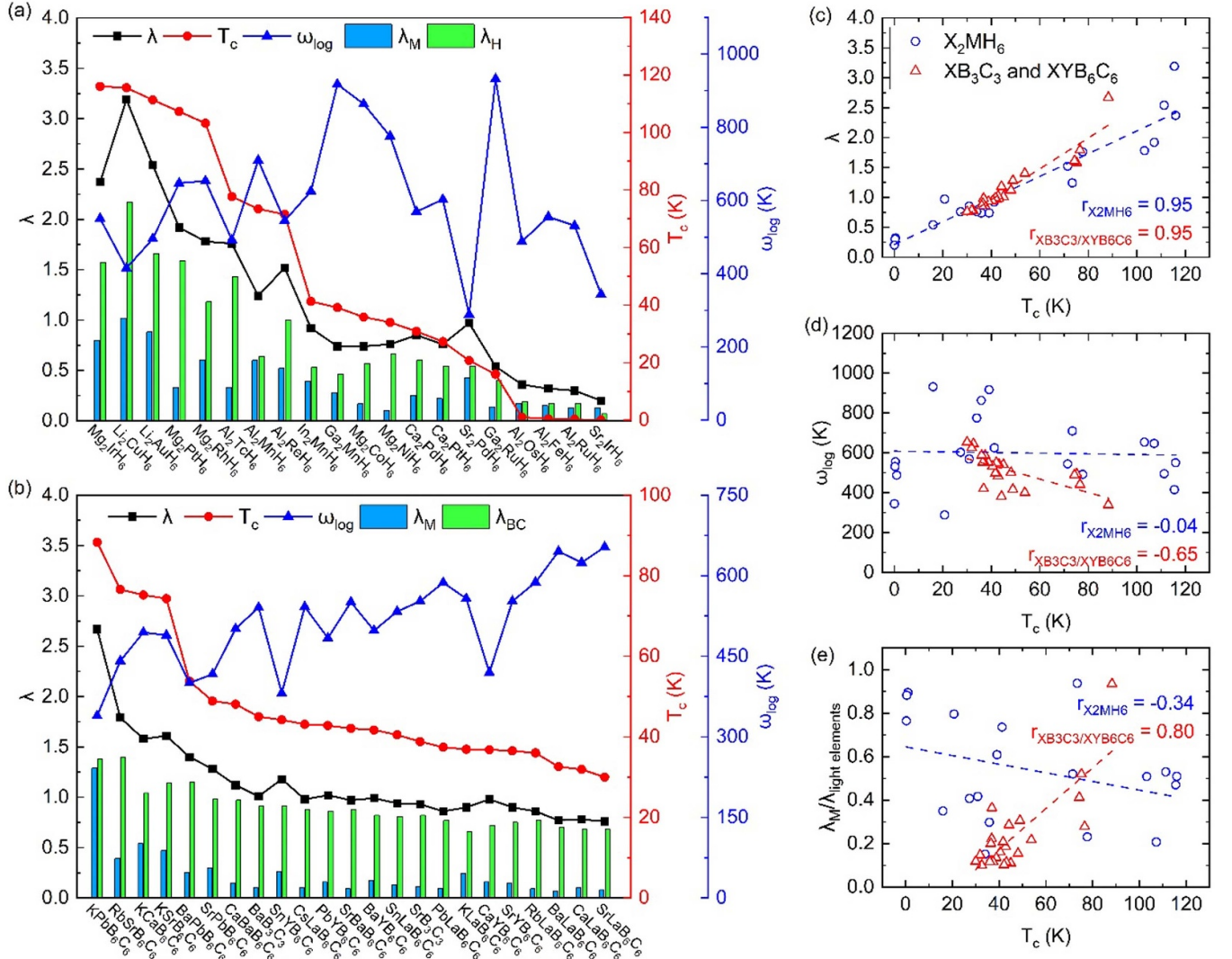


Figure 5. Calculated superconducting parameters for (a) selected X_2MH_6 compounds and (b) XB_3C_3 and XYB_6C_6 compounds. The histograms denote the EPC parameter (λ) contributed from cations (M) and light elements (H or B/C). The data of X_2MH_6 compounds were obtained with Allen-Dynes correction using coupling and shape factors [63]. The data of the XB_3C_3 and XYB_6C_6 compounds were calculated by numerically solving the Eliashberg equations [84]. (c) The correlation between λ and T_c . (d) The correlation between logarithmic average frequency (ω_{log}) and T_c . (e) Separated EPC contributions from metal and light elements (λ_M/λ_H for X_2MH_6 family and λ_M/λ_{BC} for XB_3C_3 and XYB_6C_6 family) and their correlations with T_c . r is the Pearson correlation coefficient.

in some cases, approaches $\sim 50\%$, such as in Al_2MnH_6 and $KPbB_6C_6$.

We further analyze the correlation between T_c and these superconducting parameters. Figure 5(c) suggests that λ has a very strong positive correlation with T_c in both families, as suggested by the Pearson correlation coefficient r of 0.95. In contrast, ω_{log} shows almost no correlation ($r \sim 0$) with T_c in X_2MH_6 system and a negative correlation with T_c for XB_3C_3 and XYB_6C_6 compounds, as depicted in figure 5(d). To explain the different correlations, we separate the EPC contribution between metal and light elements (H or B/C) for these compounds. In the XB_3C_3 and XYB_6C_6 families, the B–C forms a rigid bipartite sodalite clathrate structure [84]

and provides almost constant contributions to λ , as suggested by the green bars in figure 5(b). Thus, if the cation has a larger contribution to EPC, the total λ and T_c should be larger. This is demonstrated by the strong positive correlation between λ_M/λ_{BC} and T_c shown in figure 5(e). Because the cation's phonon frequencies are much lower than those of B/C, and ω_{log} represents the frequency where strong EPC occurs, a larger EPC contribution from cation leads to a smaller ω_{log} . Due to this mechanism, XB_3C_3 and XYB_6C_6 systems exhibit a strong negative correlation between ω_{log} and T_c , as shown in figure 5(d). However, in the case of X_2MH_6 system, the contributions to λ from H atoms vary among different compounds, as shown by green bars in figure 5(a). Because the phonon

spectra of X_2MH_6 can significantly change by different X and M cations, particularly the phonon bands of H [37, 62, 63], it results in a weak correlation between the λ_M/λ_H and T_c , as shown in figure 5(e). The mixed relationship among chemical elements, phonon spectra, and electron–phonon interactions weakens the correlation between ω_{\log} and T_c in X_2MH_6 system, as shown in figure 5(d). The factors that affect T_c in X_2MH_6 system are quite subtle. For instance, we found isoelectronic substitution can significantly decrease T_c , when Ir was substituted by Co (Mg_2CoH_6 with $T_c = 36$ K), or Mg was substituted by Sr (Sr_2IrH_6 with $T_c = 0$ K). The mechanism for such effect is still under investigation for this novel system [64]. These analyses demonstrate that the correlation between superconducting parameters and T_c depends on the specific system. Finding a determining parameter to describe high- T_c compounds remains a nontrivial task.

3. Experimentally synthesized superconductors

Although many ambient-pressure superconductors are computationally predicted to have high T_c , experimental realization of these superconducting systems is rare. Figure 6 shows that in the past two years, there was no major breakthrough in synthesizing high- T_c superconductors under ambient conditions. To date, MgB_2 with a T_c of 39 K [99] remains the highest among conventional ambient-pressure superconductors. Within the low-pressure range, cuprates were the only unconventional superconductors with transition temperatures exceeding the liquid nitrogen temperature range before 2023 [21]. Several experimental advancements were reported at the high-pressure regime. Figure 6 highlights a region between 140 and 200 GPa and 150–260 K, which exhibits the relatively highest T_c among the newly synthesized systems. In this range, the predicted T_c values for H_3S [100], ThH_{10} [101], CaH_6 [16], YH_9 [102], and LaH_{10} [102] closely match the experimental data [18, 20, 103–107], demonstrating excellent agreement between theory and experiment. It is worth noting that in 2023, two globally sensational room-temperature superconductors were reported: LK-99 [108] and the Lu–N–H system [109]. Despite numerous attempts by research teams to replicate these findings, none was successful [43, 48, 110–115].

At the end of 2023, Sun *et al* observed that the layered perovskite nickelate $La_3Ni_2O_7$ [130], with the $Fmmm$ space group, exhibited a high T_c of up to 80 K at 14 GPa. Zhu *et al* recently discovered SC in another Ni-based material, the trilayer $La_4Ni_3O_{10-\delta}$ single crystal, with a T_c of 30 K under 69 GPa [129]. These discoveries reignited interest in exploring the fundamental mechanisms of unconventional superconductors [131–133].

Song *et al* synthesized $LaBeH_8$ in a diamond anvil cell at pressures between 110–130 GPa, measuring a T_c of 110 K at 80 GPa [116]. This system features a La–Be framework and a novel BeH_8 unit stabilized by chemical compression from the La–Be scaffold. Inspired by $LaBeH_8$ [116], researchers predicted many alternative doped structures, including $ThBeH_8$

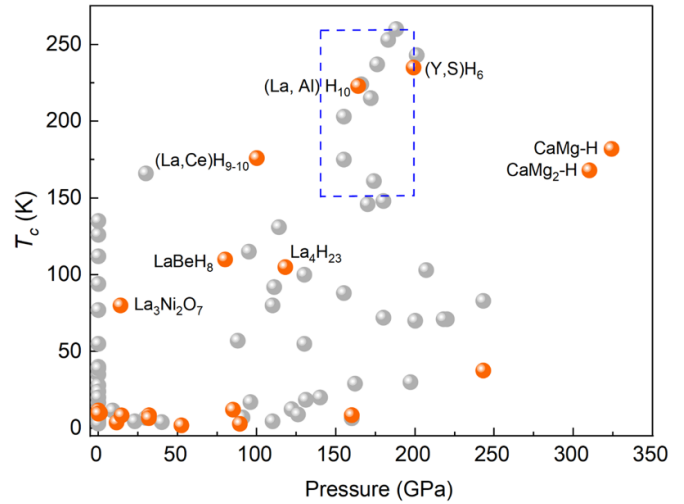


Figure 6. T_c and corresponding pressure of synthesized superconductors. The orange points represent the newly synthesized systems in 2023–2024 [116–130]. The gray points represent synthesized superconductors before 2023.

[58] ($T_c = 113$ K at 69 GPa), $CeBeH_8$ [58] ($T_c = 76$ K at 28 GPa), and $YBeH_8$ [59] ($T_c = 201$ K at 200 GPa). New quaternary superhydrides based on the supercell structure of $LaBeH_8$, such as $ThLa_3Be_4H_{32}$ ($T_c = 134$ K at 10 GPa), $LaAc_3Be_4H_{32}$ ($T_c = 135$ K at 20 GPa), and $AcLa_3Be_4H_{32}$ ($T_c = 153$ K at 20 GPa), were also proposed [40].

In the domain of high-pressure SC, LaH_{10} , synthesized in 2019 at 188 GPa, continues to hold the record with a high T_c of 260 K [107]. However, the requirement for extremely high stabilizing pressure poses significant experimental challenges. Scientists explored various methods, including element doping, to reduce the necessary pressure. For example, $(La,Al)H_{10}$ demonstrated a T_c of 223 K at 164 GPa [120], while $(La,Ce)H_{10}$ exhibited a T_c of 176 K at 100 GPa [117]. Prior theoretical investigations into LaH_{10} 's superconducting properties suggested a decrease in computed T_c values with increasing pressure [134–136], contrary to experimental findings. This inconsistency is likely due to earlier calculations overlooking minor stoichiometric defects ($LaH_{9.6}$) in the actual structure, leading to quantum diffusion effects within the rigid lanthanum lattice and resulting in a positive pressure dependence of T_c [137].

Apart from hydrides and $La_3Ni_2O_7$, most superconductors synthesized in the past two years exhibited T_c values mostly below 10 K. Examples include transition metal dichalcogenides such as $Re_{0.8}V_{0.2}Se_2$ [125] ($T_c = 3$ K at 89 GPa), $V_{0.7}Re_{0.3}Se_2$ [126] ($T_c = 4$ K at 11.5 GPa), and $PdSSe$ [124] ($T_c = 12$ K at 85 GPa); elemental superconductors Mo [121] ($T_c = 9$ K at 160 GPa) and Sc [122] ($T_c = 38$ K at 243 GPa), with Sc having the highest T_c among known elemental superconductors. Additionally, a few topological insulator superconductors were discovered, including $GeBi_2Te_4$ [127] ($T_c = 8$ K at 15 GPa), $KHgAs$ [138] ($T_c = 7$ K at 32 GPa), and $SnPSe_3$ [139] ($T_c = 9$ K at 32 GPa).

Discrepancies can sometimes exist between theoretically predicted T_c and experimentally measured T_c due to differences between theoretical models and actual experimental conditions. For instance, the predicted T_c for LiMoN_2 [36] could not be measured due to defects in the experimental structure [97]. The T_c of $(\text{La,Ce})\text{H}_{9-10}$ is difficult to accurately calculate because the computation cannot account for the configurational entropy introduced by disorder in the system [117]. The prediction for the YH_9 system was inaccurate due to a previously undiscovered experimental phase [54]. In many cases, the approach used in T_c calculation, such as the McMillan equation [10], Allen-Dynes equation [11], and Eliashberg theory [14], can yield significant variations [140]. While the most accurate T_c values should be used for comparison with experimental data, it is common to trade off accuracy for efficiency when dealing with a large number of systems. Furthermore, due to the high computational cost, the effects of anharmonicity and quantum nuclear effects are often neglected in calculations. However, these factors can also have a significant impact on T_c [141]. Anharmonic corrections alter phonon frequencies, affecting both the stability of the system and the predicted T_c , while quantum nuclear effects primarily modify the potential energy surface, potentially allowing the system to remain dynamically stable at lower pressures, thereby influencing the phase diagram. For instance, in CaH_6 , accurate T_c predictions that match experimental values are only achieved when quantum nuclear and anharmonic effects are considered using the SSCHA method [142]. Similarly, while the $Fm-3m$ phase of LaH_{10} is experimentally stable at 130 GPa, it is predicted to be unstable at 230 GPa under harmonic approximation, with anharmonic effects stabilizing it at lower pressures [136]. However, in some cases, such as LaBH_8 , anharmonic effects can destabilize the system [143]. Thus, when comparing theoretical T_c values with experimental data, it is important to examine the methods by which T_c was determined and the detailed convergence of calculations.

As previously mentioned, while many ambient-pressure superconductors are computationally predicted to have high T_c , their experimental realization remains rare. This may be due to the fact that accurately predicting synthesizability is still challenging. Most CSP are performed at 0 K, where high-temperature effects are neglected, yet these effects can be critical in synthesis experiments [144]. Moreover, even if a material is thermodynamically stable, it can still be difficult to access in experiments if there is no suitable kinetic pathway. The computational design of reaction pathways to enhance the kinetic accessibility of predicted compounds has been proven to be both possible and critical [145]. Future computational predictions should be closely integrated with experimental synthesis to form a feedback loop that enhances the synthesizability of predicted compounds. For instance, using computational design, Dolui *et al* proposed a detour in the synthesis route to the high- T_c superconductor Mg_2IrH_6 via Mg_2IrH_x [61]. Recently, Hansen *et al* successfully synthesized Mg_2IrH_5 , which may serve as a starting point to access the novel Mg_2IrH_6 phase [146].

4. Conclusions

The search for new conventional superconductors emerged as a prominent field in computational materials science. The development of advanced computational tools led to numerous predictions of new superconducting compounds in recent years, underscoring the pivotal role of computational methods in identifying potential superconductors. Currently, the focus of computational predictions shifts towards ambient pressure conditions. Among the various candidates, hydrides and boron-carbides emerged as top choices due to their promising layered and cage-like structural prototypes. The structural motifs and chemical compositions of these compounds play a crucial role in determining their superconducting properties. A critical finding is that T_c is extremely sensitive to the involved chemical elements, their compositions, and structural motifs. Isoelectronic substitutions can significantly alter T_c , highlighting the complex interplay between material composition and superconducting properties. Therefore, a data-driven approach, complemented by machine learning, remains essential to explore a broader range of chemical compositions and structures to identify high- T_c superconductors. Despite the progress in computational predictions, the experimental realization of these predicted superconductors is still lagging behind. Bridging this gap requires designing more effective synthesis routes to translate computational predictions into experimentally verified superconductors. Addressing this challenge is crucial and urgent for advancing the field and achieving practical applications of new superconducting materials.

Data availability statement

All data that support the findings of this study are included within the article (and any supplementary files).

Acknowledgments

We are grateful to W E Pickett for valuable suggestions on the manuscript. The work at Xiamen University was supported by the Natural Science Foundation of Xiamen Municipality (Grant No. 3502Z202371007), the Fundamental Research Funds for the Central Universities (Grant No. 20720230014) and the National Natural Science Foundation of China (Grant Nos. 42374108 and T2422016). The work at Jimei University was supported by the National Natural Science Foundation of China (Grant No. 12404077), the Natural Science Foundation of Xiamen Municipality (Grant No. 3502Z202372015) and the Research Foundation of Jimei University (Grant No. ZQ2023013). V A was supported by the U.S. Department of Energy, Office of Basic Energy Sciences, Division of Materials Sciences and Engineering. Ames National Laboratory is operated for the U.S. Department of Energy by Iowa State University under Contract No. DE-AC02-07CH11358. K-M H acknowledges support from National Science Foundation Award No. DMR2132666.

ORCID iDs

Feng Zheng  <https://orcid.org/0000-0001-9482-7057>
 Zhen Zhang  <https://orcid.org/0009-0001-0810-8054>
 Shunqing Wu  <https://orcid.org/0000-0002-2545-0054>
 Yang Sun  <https://orcid.org/0000-0002-4344-2920>

References

- [1] Bednorz J G and Müller K A 1986 Possible high T_c superconductivity in the Ba–La–Cu–O system *Z. Phys. B* **64** 189–93
- [2] Scalapino D J 1999 Superconductivity and spin fluctuations *J. Low Temp. Phys.* **117** 179–88
- [3] Moriya T and Ueda K 2000 Spin fluctuations and high temperature superconductivity *Adv. Phys.* **49** 555–606
- [4] Bardeen J, Cooper L N and Schrieffer J R 1957 Theory of superconductivity *Phys. Rev.* **108** 1175–204
- [5] Abrikosov A A 1962 Contribution to the theory of highly compressed matter. II *Sov. Phys. -JETP* **14** 408
- [6] De Gennes P G 1966 *Superconductivity of Metals and Alloys* (Benjamin)
- [7] Ashcroft N W 1968 Metallic hydrogen: a high-temperature superconductor? *Phys. Rev. Lett.* **21** 1748–9
- [8] Migdal A B 1958 Interaction between electrons and lattice vibrations in a normal metal *Sov. Phys. -JETP* **7** 996–1001
- [9] Eliashberg G M 1960 Interactions between electrons and lattice vibrations in a superconductor *Sov. Phys. -JETP* **11** 696–702
- [10] McMillan W L 1968 Transition temperature of strong-coupled superconductors *Phys. Rev.* **167** 331–44
- [11] Dynes R C 1972 McMillan's equation and the T_c of superconductors *Solid State Commun.* **10** 615–8
- [12] Allen P B and Dynes R C 1975 Transition temperature of strong-coupled superconductors reanalyzed *Phys. Rev. B* **12** 905–22
- [13] Oliveira L N, Gross E K U and Kohn W 1988 Density-functional theory for superconductors *Phys. Rev. Lett.* **60** 2430–3
- [14] Margine E R and Giustino F 2013 Anisotropic migdal-eliasberg theory using wannier functions *Phys. Rev. B* **87** 024505
- [15] Lilia B *et al* 2022 The 2021 room-temperature superconductivity roadmap *J. Phys.: Condens. Matter* **34** 183002
- [16] Wang H, Tse J S, Tanaka K, Iitaka T and Ma Y 2012 Superconductive sodalite-like clathrate calcium hydride at high pressures *Proc. Natl Acad. Sci.* **109** 6463–6
- [17] Troyan I A *et al* 2021 Anomalous high-temperature superconductivity in YH_6 *Adv. Mater.* **33** 2006832
- [18] Kong P P *et al* 2019 Superconductivity up to 243 K in yttrium hydrides under high pressure *Nat. Commun.* **12** 5075
- [19] Liu H, Naumov I I, Hoffmann R, Ashcroft N W and Hemley R J 2017 Potential high- T_c superconducting lanthanum and yttrium hydrides at high pressure *Proc. Natl Acad. Sci.* **114** 6990–5
- [20] Drozdov A P *et al* 2019 Superconductivity at 250 K in lanthanum hydride under high pressures *Nature* **569** 528–31
- [21] Sun Y, Zhong X, Liu H and Ma Y 2023 Clathrate metal superhydrides at high-pressure conditions: enroute to room-temperature superconductivity *Natl Sci. Rev.* **11** nwad270
- [22] Atchley S *et al* 2023 Frontier: exploring exascale the system architecture of the first exascale supercomputer *SC23: Int. Conf. for High Performance Computing, Networking, Storage and Analysis* pp 1–16
- [23] Mann A 2020 Nascent exascale supercomputers offer promise, present challenges *Proc. Natl Acad. Sci.* **117** 22623–5
- [24] Young D J, Chu A, Song E Y, Barberena D, Wellnitz D, Niu Z, Schäfer V M, Lewis-Swan R J, Rey A M and Thompson J K 2024 Observing dynamical phases of BCS superconductors in a cavity QED simulator *Nature* **625** 679–84
- [25] Li X *et al* 2024 Observation and quantification of the pseudogap in unitary Fermi gases *Nature* **626** 288–93
- [26] Wang Y, Lv J, Zhu L and Ma Y 2012 CALYPSO: a method for crystal structure prediction *Comput. Phys. Commun.* **183** 2063–70
- [27] Glass C W, Oganov A R and Hansen N 2006 USPEX-evolutionary crystal structure prediction *Comput. Phys. Commun.* **175** 713–20
- [28] Pickard C J and Needs R J 2011 *Ab initio* random structure searching *J. Phys.: Condens. Matter* **23** 053201
- [29] Wines D, Choudhary K, Biacchi A J, Garrity K F and Tavazza F 2023 High-throughput DFT-based discovery of next generation two-dimensional (2D) superconductors *Nano Lett.* **23** 969–78
- [30] Chen S, Wu Z, Zhang Z, Wu S, Ho K-M, Antropov V and Sun Y 2024 High-throughput screening for boride superconductors *Inorg. Chem.* **63** 8654–63
- [31] Zheng F, Sun Y, Wang R, Fang Y, Zhang F, Wu S, Lin Q, Wang C-Z, Antropov V and Ho K-M 2023 Prediction of superconductivity in metallic boron–carbon compounds from 0 to 100 GPa by high-throughput screening *Phys. Chem. Chem. Phys.* **25** 32594–601
- [32] Song J, Qin Y, Shi D, Chen X, Li W, Ren R, Wang Y, Yang X and Cao C 2024 A high-throughput screening and discovery of lanthanum based ternary noncentrosymmetric superconductors with ZrNiAl -structure from *ab initio* calculations *J. Phys. Chem. Solids* **184** 111676
- [33] Pickett W E 2023 Colloquium: room temperature superconductivity: the roles of theory and materials design *Rev. Mod. Phys.* **95** 021001
- [34] Zhang L, Wang Y, Lv J and Ma Y 2017 Materials discovery at high pressures *Nat. Rev. Mater.* **2** 17005
- [35] Xie H *et al* 2020 Hydrogen pentagraphenelike structure stabilized by hafnium: a high-temperature conventional superconductor *Phys. Rev. Lett.* **125** 217001
- [36] Cerqueira T F T, Sanna A and Marques M A L 2024 Sampling the materials space for conventional superconducting compounds *Adv. Mater.* **36** 2307085
- [37] Cerqueira T F T, Fang Y-W, Errea I, Sanna A and Marques M A L 2024 Searching materials space for hydride superconductors at ambient pressure *Adv. Funct. Mater.* **34** 2404043
- [38] He Y and Shi J 2023 Few-hydrogen High- T_c superconductivity in $(\text{Be}_4)_2\text{H}$ nanosuperlattice with promising ductility under ambient pressure *Nano Lett.* **23** 8126–31
- [39] Huo Z, Duan D, Jiang Q, Zhang Z and Cui T 2023 Cubic H_3S stabilized by halogens: high-temperature superconductors at mild pressure *Sci. China Phys. Mech. Astron.* **66** 118211
- [40] Zhao W, Duan D, An D, Jiang Q, Liu Z, Ma T, Du J and Cui T 2024 High temperature superconductivity of quaternary hydrides $\text{XM}_3\text{Be}_4\text{H}_{32}$ ($\text{X}, \text{M} = \text{Ca}, \text{Sr}, \text{Ba}, \text{Y}, \text{La}, \text{Ac}, \text{Th}$) under moderate pressure *Mater. Today Phys.* **43** 101387
- [41] Gao K, Cui W, Shi J, Durajski A P, Hao J, Botti S, Marques M A L and Li Y 2024 Prediction of high- T_c superconductivity in ternary actinium beryllium hydrides at low pressure *Phys. Rev. B* **109** 014501
- [42] Liang X, Wei X, Zurek E, Bergara A, Li P, Gao G and Tian Y 2024 Design of high-temperature superconductors at

- moderate pressures by alloying AlH_3 or GaH_3 *Matter Radiat. Extremes* **9** 018401
- [43] Fang Y-W, Dangić D and Errea I 2024 Assessing the feasibility of near-ambient conditions superconductivity in the Lu-N-H system *Commun. Mater.* **5** 61
- [44] Lucrezi R, Kogler E, Di Cataldo S, Aichhorn M, Boeri L and Heil C 2023 Quantum lattice dynamics and their importance in ternary superhydride clathrates *Commun. Phys.* **6** 298
- [45] Liu P, Zhao W, Liu Z, Pan Y, Duan D and Cui T 2024 High-temperature superconductivities and crucial factors influencing the stability of LaThH_{12} under moderate pressures *Phys. Chem. Chem. Phys.* **26** 8237–46
- [46] Wang Q, Zhang S, Li H, Wang H, Liu G, Ma J, Xu H, Liu H and Ma Y 2023 Coexistence of superconductivity and electride states in Ca_2H with an antiferrotype motif under compression *J. Mater. Chem. A* **11** 21345–53
- [47] Xu M, Duan D, Du M, Zhao W, An D, Song H and Cui T 2023 Phase diagrams and superconductivity of ternary Ca-Al-H compounds under high pressure *Phys. Chem. Chem. Phys.* **25** 32534–40
- [48] Huo Z, Duan D, Ma T, Zhang Z, Jiang Q, An D, Song H, Tian F and Cui T 2023 First-principles study on the conventional superconductivity of N-doped *fcc*- LuH_3 *Matter Radiat. Extremes* **8** 038402
- [49] Huang H, Deng C, Song H, Du M, Duan D, Liu Y and Cui T 2024 Superconductivity of thulium substituted clathrate hexahydrides at moderate pressure *Sci. Rep.* **14** 10729
- [50] Jiang Q, Duan D, Song H, Zhang Z, Huo Z, Cui T and Yao Y 2023 Room temperature superconductivity in ScH_{12} with quasi-atomic hydrogen below megabar pressure (arXiv:2302.02621)
- [51] Wang Y, Chen S, Guo J, Huang X and Cui T 2024 Absence of superconductivity in *I4/mmm*- FeH_5 : experimental evidence *Phys. Chem. Chem. Phys.* **26** 7371–6
- [52] Zhao W, Song H, Du M, Jiang Q, Ma T, Xu M, Duan D and Cui T 2023 Pressure-induced high-temperature superconductivity in ternary Y-Zr-H compounds *Phys. Chem. Chem. Phys.* **25** 5237–43
- [53] He X-L, Zhang P, Ma Y, Li H, Zhong X, Wang Y, Liu H and Ma Y 2023 Potential high-temperature superconductivity in the substitutional alloy of (Y, Sr) H_{11} under high pressure *Phys. Rev. B* **107** 134509
- [54] Du M, Li Z, Duan D and Cui T 2023 Superconducting phases of YH_9 under pressure *Phys. Rev. B* **108** 174507
- [55] Geng N, Hilleke K P, Belli F, Das P K and Zurek E 2024 Superconductivity in CH_4 and BH_4 -containing compounds derived from the high-pressure superhydrides *Mater. Today Phys.* **44** 101443
- [56] An D, Duan D, Zhang Z, Jiang Q, Song H and Cui T 2023 Thermodynamically stable room-temperature superconductors in Li-Na hydrides under high pressures (arXiv:2303.09805)
- [57] Liu X, Zhang L, Wang M, Huang X, Liu L and Jia Y 2024 Realizing high T_c ambient-pressure superconductivity in hole-doped hydride $\text{Mg}(\text{BH}_4)_2$ *Mater. Today Phys.* **40** 101299
- [58] Jiang Q, Zhang Z, Song H, Ma Y, Sun Y, Miao M, Cui T and Duan D 2024 Ternary superconducting hydrides stabilized via Th and Ce elements at mild pressures *Fundam. Res.* **4** 550–6
- [59] Du J, Jiang Q, Zhang Z, Zhao W, Chen L, Huo Z, Song H, Tian F, Duan D and Cui T 2024 First-principles study of high-pressure structural phase transition and superconductivity of YBeH_8 *J. Chem. Phys.* **160** 094116
- [60] Fan Y, Li B, Zhu C, Cheng J, Liu S and Shi Z 2024 Superconductive sodalite-like clathrate hydrides MXH_{12} with critical temperatures of near 300 K under pressures *Phys. Status Solidi b* **2400240**
- [61] Dolui K, Conway L J, Heil C, Strobel T A, Prasankumar R P and Pickard C J 2024 Feasible route to high-temperature ambient-pressure hydride superconductivity *Phys. Rev. Lett.* **132** 166001
- [62] Sanna A, Cerqueira T F T, Fang Y-W, Errea I, Ludwig A and Marques M A L 2024 Prediction of ambient pressure conventional superconductivity above 80 K in hydride compounds *npj Comput. Mater.* **10** 44
- [63] Zheng F, Zhang Z, Wu S, Lin Q, Wang R, Fang Y, Wang C-Z, Antropov V, Sun Y and Ho K-M 2024 Prediction of ambient pressure superconductivity in cubic ternary hydrides with MH_6 octahedra *Mater. Today Phys.* **42** 101374
- [64] Wang X, Pickett W, Hutcheon M, Prasankumar R and Zurek E 2024 Why Mg_2IrH_6 is predicted to be a high temperature superconductor, but Ca_2IrH_6 is not (arXiv:2407.10889)
- [65] Di Cataldo S and Boeri L 2023 Metal borohydrides as ambient-pressure high- T_c superconductors *Phys. Rev. B* **107** L060501
- [66] He T *et al* 2001 Superconductivity in the non-oxide perovskite MgCNi_3 *Nature* **411** 54–56
- [67] Singh D J and Mazin I I 2001 Superconductivity and electronic structure of perovskite MgCNi_3 *Phys. Rev. B* **64** 140507
- [68] Tian C, He Y, Zhu Y, Du J, Liu S, Guo W, Zhong H, Lu J, Wang X and Shi J 2024 Few-hydrogen metal-bonded perovskite superconductor MgHCu_3 with a critical temperature of 42 K under atmospheric pressure *Adv. Funct. Mater.* **34** 2304919
- [69] Ikeda K, Sato T and Orimo S 2008 Perovskite-type hydrides-synthesis, structures and properties *Int. J. Mater. Res.* **99** 471–9
- [70] Gao S *et al* 2021 Hydride-based antiperovskites with soft anionic sublattices as fast alkali ionic conductors *Nat. Commun.* **12** 201
- [71] Kamegawa A, Abiko T and Okada M 2014 High-pressure synthesis of novel hydrides and intermetallic compound in Al-X systems (X= Sr, V, Hf) *Mater. Sci. Forum* **783–786** 1686–91
- [72] Jia C, Li X, Li Q and Yang J 2023 Hydrogen anion as a strong magnetic mediator for obtaining high-temperature ferromagnetic semiconductors: the case of hydride double perovskites *Phys. Rev. B* **107** L140404
- [73] Gao M, Yan X-W, Lu Z-Y and Xiang T 2021 Phonon-mediated high-temperature superconductivity in the ternary borohydride KB_2H_8 under pressure near 12 GPa *Phys. Rev. B* **104** L100504
- [74] Li S, Wang H, Sun W, Lu C and Peng F 2022 Superconductivity in compressed ternary alkaline boron hydrides *Phys. Rev. B* **105** 224107
- [75] Tomassetti C R, Kafle G P, Marcial E T, Margine E R and Kolmogorov A N 2024 Prospect of high-temperature superconductivity in layered metal borocarbides *J. Mater. Chem. C* **12** 4870–84
- [76] Wörle M, Nesper R, Mair G, Schwarz M and Von Schnering H G 1995 LiBC-ein vollständig interkalierter Heterographit *Z. Anorg. Allg. Chem.* **621** 1153–9
- [77] Karimov P F, Skorikov N A, Kurmaev E Z, Finkelstein L D, Leitch S, MacNaughton J, Moewes A and Mori T 2004 Resonant inelastic soft x-ray scattering and electronic structure of LiBC *J. Phys.: Condens. Matter* **16** 5137
- [78] Rosner H, Kitaigorodsky A and Pickett W E 2002 Prediction of high T_c superconductivity in hole-doped LiBC *Phys. Rev. Lett.* **88** 127001
- [79] Miao R, Yang J, Jiang M, Zhang Q, Cai D, Fan C, Bai Z, Liu C, Wu F and Ma S 2013 First-principles study of superconductivity in the hole self-doped $\text{LiB}_{1.1}\text{C}_{0.9}$ *J. Appl. Phys.* **113** 133910

- [80] Gao M, Lu Z-Y and Xiang T 2015 Prediction of phonon-mediated high-temperature superconductivity in $\text{Li}_3\text{B}_4\text{C}_2$ *Phys. Rev. B* **91** 045132
- [81] Zheng F, Sun Y, Wang R, Fang Y, Zhang F, Wu S, Wang C-Z, Antropov V and Ho K-M 2023 Superconductivity in the Li-B-C system at 100 GPa *Phys. Rev. B* **107** 014508
- [82] Laranjeira J, Errea I, Dangic D, Marques L, Melle-Franco M and Strutynski K 2023 Superconductivity in the doped polymerized fullerite clathrate from first principles *Rapid Res. Lett.* **18** 2300249
- [83] Xie H, Wang H, Qin F, Han W, Wang S, Wang Y, Tian F and Duan D 2023 A fresh class of superconducting and hard pentaborides *Matter Radiat. Extremes* **8** 058404
- [84] Geng N, Hilleke K P, Zhu L, Wang X, Strobel T A and Zurek E 2023 Conventional high-temperature superconductivity in metallic, covalently bonded, binary-guest C-B clathrates *J. Am. Chem. Soc.* **145** 1696–706
- [85] Duan Q, Zhan L, Shen J, Zhong X and Lu C 2024 Predicting superconductivity near 70 K in 1166-type boron-carbon clathrates at ambient pressure *Phys. Rev. B* **109** 054505
- [86] Li B, Cheng Y, Zhu C, Cheng J and Liu S 2024 Superconductivity near 70 K in boron-carbon clathrates MB_2C_8 (M=Na, K, Rb, Cs) at ambient pressure *Phys. Rev. B* **109** 184517
- [87] Schmidt J, Hoffmann N, Wang H, Borlido P, Carriço P J M A, Cerqueira T F T, Botti S and Marques M A L 2023 Machine-learning-assisted determination of the global zero-temperature phase diagram of materials *Adv. Mater.* **35** 2210788
- [88] Zhu L *et al* 2020 Carbon-boron clathrates as a new class of sp^3 -bonded framework materials *Sci. Adv.* **6** eaay8361
- [89] Di Cataldo S, Qulaghasi S, Bachelet G B and Boeri L 2022 High- T_c superconductivity in doped boron-carbon clathrates *Phys. Rev. B* **105** 064516
- [90] Wang J-N, Yan X-W and Gao M 2021 High-temperature superconductivity in SrB_3C_3 and BaB_3C_3 predicted from first-principles anisotropic migdal-eliasberg theory *Phys. Rev. B* **103** 144515
- [91] Zhu L *et al* 2023 Superconductivity in SrB_3C_3 clathrate *Phys. Rev. Res.* **5** 013012
- [92] Cui Z, Zhang X, Sun Y, Liu Y and Yang G 2022 Prediction of novel boron-carbon based clathrates *Phys. Chem. Chem. Phys.* **24** 16884–90
- [93] Gai T-T, Guo P-J, Yang H-C, Gao Y, Gao M and Lu Z-Y 2022 Van Hove singularity induced phonon-mediated superconductivity above 77 K in hole-doped SrB_3C_3 *Phys. Rev. B* **105** 224514
- [94] Zhang P, Li X, Yang X, Wang H, Yao Y and Liu H 2022 Path to high- T_c superconductivity via Rb substitution of guest metal atoms in the SrB_3C_3 clathrate *Phys. Rev. B* **105** 094503
- [95] Tomassetti C R, Gochitashvili D, Renskers C, Margine E R and Kolmogorov A N 2024 First-principles design of ambient-pressure $\text{Mg}_x\text{B}_2\text{C}_2$ and Na_xBC superconductors (arXiv:2407.09347)
- [96] Yang X, Zhao W, Ma L, Lu W, Zhong X, Xie Y, Liu H and Ma Y 2023 Prediction of fully metallic σ -bonded boron framework induced high superconductivity above 100 K in thermodynamically stable Sr_2B_5 at 40 GPa (arXiv:2310.13945)
- [97] Elder S H, Doerr L H, DiSalvo F J and Parise J B 1992 LiMoN_2 : the first metallic layered nitride *Chem. Mater.* **4** 928–37
- [98] Hoffmann N, Cerqueira T F T, Borlido P, Sanna A, Schmidt J and Marques M A L 2023 Searching for ductile superconducting heusler X_2YZ compounds *npj Comput. Mater.* **9** 138
- [99] Nagamatsu J, Nakagawa N, Muranaka T, Zenitani Y and Akimitsu J 2001 Superconductivity at 39 K in magnesium diboride *Nature* **410** 63–64
- [100] Duan D, Huang X, Tian F, Li D, Yu H, Liu Y, Ma Y, Liu B and Cui T 2015 Pressure-induced decomposition of solid hydrogen sulfide *Phys. Rev. B* **91** 180502
- [101] Kvashnin A G, Semenov D V, Kruglov I A, Wrona I A and Oganov A R 2018 High-temperature superconductivity in a Th–H system under pressure conditions *ACS Appl. Mater. Interfaces* **10** 43809–16
- [102] Peng F, Sun Y, Pickard C J, Needs R J, Wu Q and Ma Y 2017 Hydrogen clathrate structures in rare earth hydrides at high pressures: possible route to room-temperature superconductivity *Phys. Rev. Lett.* **119** 107001
- [103] Semenov D V, Kvashnin A G, Ivanova A G, Svitlyk V, Yu Fominski V, Sadakov A V, Sobolevskiy O A, Pudalov V M, Troyan I A and Oganov A R 2020 Superconductivity at 161 K in thorium hydride ThH_{10} : synthesis and properties *Mater. Today* **33** 36–44
- [104] Ma L *et al* 2022 High-temperature superconducting phase in clathrate calcium hydride CaH_6 up to 215 K at a pressure of 172 GPa *Phys. Rev. Lett.* **128** 167001
- [105] Li Z *et al* 2022 Superconductivity above 200 K discovered in superhydrides of calcium *Nat. Commun.* **13** 2863
- [106] Wang Y, Wang K, Sun Y, Ma L, Wang Y, Zou B, Liu G, Zhou M and Wang H 2022 Synthesis and superconductivity in yttrium superhydrides under high pressure *Chinese Phys. B* **31** 106201
- [107] Somayazulu M, Ahart M, Mishra A K, Geballe Z M, Baldini M, Meng Y, Struzhkin V V and Hemley R J 2019 Evidence for superconductivity above 260 K in lanthanum superhydride at megabar pressures *Phys. Rev. Lett.* **122** 027001
- [108] Lee S, Kim J-H and Kwon Y-W 2023 The first room-temperature ambient-pressure superconductor (arXiv:2307.12008)
- [109] Dasenbrock-Gammon N *et al* 2023 RETRACTED ARTICLE: evidence of near-ambient superconductivity in a N-doped lutetium hydride *Nature* **615** 244–50
- [110] Xing X *et al* 2023 Observation of non-superconducting phase changes in nitrogen doped lutetium hydrides *Nat. Commun.* **14** 5991
- [111] Ferreira P P, Conway L J, Cucciari A, Di Cataldo S, Giannessi F, Kogler E, Eleno L T F, Pickard C J, Heil C and Boeri L 2023 Search for ambient superconductivity in the Lu–N–H system *Nat. Commun.* **14** 5367
- [112] Hilleke K P, Wang X, Luo D, Geng N, Wang B and Zurek E 2023 Structure, stability and superconductivity of N-doped lutetium hydrides at kbar pressures *Phys. Rev. B* **108** 014511
- [113] Korotin D M, Novoselov D Y, Shorikov A O, Anisimov V I and Oganov A R 2023 Electronic correlations in the ultranarrow energy band compound $\text{Pb}_9\text{Cu}(\text{PO}_4)_6\text{O}$: a DFT + DMFT study *Phys. Rev. B* **108** L241111
- [114] Kim S-W, Wang K, Chen S, Conway L J, Pascut G L, Errea I, Pickard C J and Monserrat B 2024 On the dynamical stability of copper-doped lead apatite *npj Comput. Mater.* **10** 16
- [115] Kim S-W, Conway L J, Pickard C J, Pascut G L and Monserrat B 2023 Microscopic theory of colour in lutetium hydride *Nat. Commun.* **14** 7360
- [116] Song Y, Bi J, Nakamoto Y, Shimizu K, Liu H, Zou B, Liu G, Wang H and Ma Y 2023 Stoichiometric ternary superhydride LaBeH_8 as a new template for high-temperature superconductivity at 110 K under 80 GPa *Phys. Rev. Lett.* **130** 266001
- [117] Chen W, Huang X, Semenov D V, Chen S, Zhou D, Zhang K, Oganov A R and Cui T 2023 Enhancement of

- superconducting properties in the La-Ce-H system at moderate pressures *Nat. Commun.* **14** 2660
- [118] Zhang K, Chen W, Zhang Y, Guo J, Chen S, Huang X and Cui T 2024 High-pressure synthesis of a ternary yttrium-sulfur hydride superconductor with a high T_c of approximately 235 K *Sci. China Phys. Mech. Astron.* **67** 238211
- [119] Guo J, Semenok D, Shutov G, Zhou D, Chen S, Wang Y, Helm T, Huang X and Cui T 2024 Large negative magnetoresistance and pseudogap phase in superconducting A15-type La_4H_{23} *Natl Sci. Rev.* **11** nwae149
- [120] Chen S, Qian Y, Huang X, Chen W, Guo J, Zhang K, Zhang J, Yuan H and Cui T 2023 High-temperature superconductivity up to 223 K in the Al stabilized metastable hexagonal lanthanum superhydride *Natl Sci. Rev.* **11** nwad107
- [121] Wu X *et al* 2024 Robust T_c in element molybdenum up to 160 GPa *Chinese Phys. B* **33** 047406
- [122] Wang K, Sun Y, Zhou M, Liu H, Ma G, Wang H, Liu G and Ma Y 2023 Superconductivity up to 37.6 K in compressed scandium *Phys. Rev. Res.* **5** 043248
- [123] Sanchez J J *et al* 2023 Strain-switchable field-induced superconductivity *Sci. Adv.* **9** eadj5200
- [124] Liu S, Zhao X, Song H, Lv X, Chen J, Dan Y, Huang Y and Cui T 2024 Experimental investigation of superconductivity in PdSSe under high pressure *Adv. Electr. Mater.* **10** 2300707
- [125] Tian C, Gao Y, Huang X, Fang Y, Huang F and Cui T 2023 Giant reduction of stabilized pressure for the superconducting $\text{Re}_{0.8}\text{V}_{0.2}\text{Se}_2$ phase *Inorg. Chem.* **62** 11626–32
- [126] Tian C, Huang X, Gao Y, Tian F, Liang M, Fang Y, Huang F and Cui T 2023 Multiband superconducting state and Lifshitz transition in $\text{V}_{0.7}\text{Re}_{0.3}\text{Se}_2$ at high pressure *Phys. Rev. B* **108** L180507
- [127] Liu C, Gao Y, Tian C, Jiang C, Zhu C, Wu X, Huang X and Cui T 2024 Pressure-driven dome-shaped superconductivity in topological insulator GeBi_2Te_4 *J. Phys.: Condens. Matter* **36** 225703
- [128] Kuzovnikov M A, Antonov V E, Kulakov V I, Muzalevsky V D, Orlov N S, Palnichenko A V and Shulga Y M 2023 Synthesis of superconducting hcp-ZrH₃ under high hydrogen pressure *Phys. Rev. Mater.* **7** 024803
- [129] Zhu Y *et al* 2024 Superconductivity in pressurized trilayer $\text{La}_4\text{Ni}_3\text{O}_{10-\delta}$ single crystals *Nature* **631** 531–6
- [130] Sun H *et al* 2023 Signatures of superconductivity near 80 K in a nickelate under high pressure *Nature* **621** 493–8
- [131] Chen X *et al* 2024 Polymorphism in the ruddlesden-popper nickelate $\text{La}_3\text{Ni}_2\text{O}_7$: discovery of a hidden phase with distinctive layer stacking *J. Am. Chem. Soc.* **146** 3640–5
- [132] Wang L *et al* 2024 Structure responsible for the superconducting state in $\text{La}_3\text{Ni}_2\text{O}_7$ at high-pressure and low-temperature conditions *J. Am. Chem. Soc.* **146** 7506–14
- [133] Wang H, Chen L, Rutherford A, Zhou H and Xie W 2024 Long-range structural order in a hidden phase of ruddlesden-popper bilayer nickelate $\text{La}_3\text{Ni}_2\text{O}_7$ *Inorg. Chem.* **63** 5020–6
- [134] Liu L, Wang C, Yi S, Kim K W, Kim J and Cho J-H 2019 Microscopic mechanism of room-temperature superconductivity in compressed LaH_{10} *Phys. Rev. B* **99** 140501
- [135] Wang C, Yi S and Cho J-H 2019 Pressure dependence of the superconducting transition temperature of compressed LaH_{10} *Phys. Rev. B* **100** 060502
- [136] Errea I *et al* 2020 Quantum crystal structure in the 250 kelvin superconducting lanthanum hydride *Nature* **578** 66–69
- [137] Wang H, Salzbrenner P T, Errea I, Peng F, Lu Z, Liu H, Zhu L, Pickard C J and Yao Y 2023 Quantum structural fluxion in superconducting lanthanum polyhydride *Nat. Commun.* **14** 1674
- [138] Dai G *et al* 2023 Pressure-induced superconductivity in the nonsymmorphic topological insulator KHgAs *NPG Asia Mater.* **15** 52
- [139] Qi M, Chen W, Huang Y, Song H, Lv X, Wu M, Zhao W, Zhang L and Cui T 2024 Pressure-induced superconductivity in van der Waals layered semiconductor SnPSe_3 *J. Mater. Chem. C* **12** 5108–13
- [140] Kaffle G P, Tomassetti C R, Mazin I I, Kolmogorov A N and Margine E R 2022 *Ab initio* study of Li-Mg-B superconductors *Phys. Rev. Mater.* **6** 084801
- [141] Setty C, Baggioli M and Zaccone A 2024 Anharmonic theory of superconductivity and its applications to emerging quantum materials *J. Phys.: Condens. Matter* **36** 173002
- [142] Hou P, Huo Z and Duan D 2023 Quantum and anharmonic effects in superconducting $1m\text{-}3m$ CaH_6 under high pressure: a first-principles study *J. Phys. Chem. C* **127** 23980–7
- [143] Belli F and Errea I 2022 Impact of ionic quantum fluctuations on the thermodynamic stability and superconductivity of LaBH_8 *Phys. Rev. B* **106** 134509
- [144] Kruglov I A, Yanilkin A V, Propad Y, Mazitov A B, Rachitskii P and Oganov A R 2023 Crystal structure prediction at finite temperatures *npj Comput. Mater.* **9** 1–8
- [145] Szymanski N J *et al* 2023 An autonomous laboratory for the accelerated synthesis of novel materials *Nature* **624** 86–91
- [146] Hansen M F, Conway L J, Dolui K, Heil C, Pickard C J, Mezouar M, Kunz M, Prasankumar R P and Strobel T A 2024 Synthesis of Mg_2IrH_5 : a potential pathway to high- T_c hydride superconductivity at ambient pressure (arXiv:2406.09538)